Electrical Power and Energy Systems 132 (2021) 107154

Contents lists available at ScienceDirect

International Journal of Electrical Power and Energy Systems

journal homepage: www.elsevier.com/locate/ijepes

Model reduction and feedback design based on singular perturbation method applied to a lumped DER-microgrid model

Bruno Salgado Bizzo [a], Guilherme Araujo Pimentel [a,b,*], Rafael da Silveira Castro [a], Ricardo Pérez-Ibacache [a,c]

[a] Group of Automation and Control Systems (GACS) - School of Technology, Pontifical Catholic University of Rio Grande do Sul, Brazil
[b] Systems, Estimation, Control and Optimization Group (SECO), University of Mons, Mons, Belgium
[c] Andes Volt Industrial, Los Rios, Valdivia, Chile

ARTICLE INFO

Keywords:
Distributed energy resources
Microgrid
Order reduction
Singular perturbation

ABSTRACT

In the context of microgrids, the distributed energy resources (DERs) are interfaced through an LCL output filter with the rest of the microgrid. The dynamic model of this filter and the lumped model of the microgrid constitute the set of differential equations employed to design the controller that allows the integration of DER units within the modern power systems. For those control strategies based on cascade structure; shunt capacitor voltage (inner) and droop (outer) controllers, it is important to specify under which conditions the model reduction is authorized. In this work, the singular perturbation method is used to derive the conditions that allow a model reduction of the output filter. In addition, two case studies are presented to illustrate the applicability and the possibility of model reduction.

1. Introduction

The dominant modes of conventional electrical power systems have historically been associated with the electromechanical responses of synchronous machines. These modes are significantly slower than those associated with electromagnetic responses of networks and transformers. Therefore, these faster modes could be neglected in a general analysis. This approximation is well known and constitutes a model reduction that has successfully been applied in practice [1,2]. With the modernization of the electrical power system (microgrid deployment), a considerable amount of power will be supplied by inverter-based Distributed Energy Resources (DERs), such as solar panels, wind turbines, and energy storage. One of the main characteristics of these DER units is that, in general, they are connected to a medium- or low-voltage distribution network. As DER units and distribution networks exhibit modes of similar time-scale, the use of an approach based on a model reduction to characterize the dominant dynamics needs to be reexamined [3].

The operation of electrical power systems, including the microgrids, is mainly structured in two control levels: (i) decentralized and (ii) centralized controllers. The decentralized controller (or primary) deals with the stability and resilience of the network, and the centralized controller (or secondary and tertiary) is responsible for the efficiency and reliability of the power system. In order to interface the DER units within a microgrid, decentralized controllers require to be designed. Such design is based on a dynamic model, that describes the interaction between the DER unit and the whole microgrid seen at the Point of Connection (PoC) of the DER unit, from now on called a DER-microgrid model. Such a model is intrinsically difficult to obtain, mainly because of the proximity in the time-scale of the involved variables. A frequent approach in the control of DER units is to inherit, from the conventional power systems, its control structure and design; in particular, cascade control structures and closed-loop design based on droop gains [4,5]. As the dynamic responses of the DER units and the elements that constitute the electrical network may reside in a similar time-scale, the assumptions from the conventional power systems may not be longer valid. Therefore, the main aim of this study is to revisit the limitations that impose a DER-microgrid dynamic model that precedes the decentralized closed-loop structure and design decision.

The most recent researches on integrating DER units into a microgrid were introduced in [6–9], where an effort was made to find a reduced model for the DER unit, for stability analysis of a microgrid. All these

* Corresponding author at: Systems, Estimation, Control and Optimization Group (SECO), University of Mons, Mons, Belgium
E-mail addresses: bruno.bizzo@edu.pucrs.br (B.S. Bizzo), guilherme.araujopimentel@umons.ac.be (G.A. Pimentel), rafael.castro@pucrs.br (R. da Silveira Castro), rperez@unmanned.cl (R. Pérez-Ibacache).

https://doi.org/10.1016/j.ijepes.2021.107154
Received 15 August 2020; Received in revised form 27 February 2021; Accepted 24 March 2021
Available online 19 May 2021

studies concluded that the dynamics involved between the DER unit and the microgrid are on a similar time-scale. For a particular DER unit closed-loop design, they propose a model reduction that disregards the effect of the operating conditions and/or relationships between parameters, which may or may not allow the reduction of the model in an open or closed loop. It implies that the model reduction based on the previous proposals is sensitive to a particular set of parameters and closed loop design. Additionally, in regard to the controller synthesis, the aforementioned studies were based on the linearized DER-microgrid model. However, such linearization around the point of operation is only possible for a limited number of classes of models represented by differential equations. Because of these two aspects, the nonlinearities and its model reduction have been frequently overlooked in the current literature, perhaps because of the complexity in dealing with the nonlinearities. Because of that, theoretical analysis methodologies can be used as an attempt to predict — regionally and globally — the approximate behavior of a non-linear system. One of these methods is the singular perturbation method.

The singular perturbation method, classified also as an asymptotic analysis method for differential equations, offers an approximate solution of the original nonlinear system. This method decomposes the original system into two or more smaller subsystems, which can be analyzed separately. The application of the singular perturbation method results in the identification of the underlying properties of the original nonlinear system representation, revealing, in many cases, structures with multiple time-scales, inherent to many practical problems [10]. The study of its intrinsic properties is not an easy task, in particular for complex physical systems, as the microgrids [11]. Nonetheless, in the current work, some assumptions mentioned in the literature are relaxed, allowing for a more representative theoretical analysis of the time-scales involved in a DER-microgrid interaction model.

The contribution of this paper is threefold: (i) to establish conditions for decoupling variables and reducing the order of the nonlinear DER-microgrid model based on the system physical compounds, (ii) to analytically design a decentralized control of the DER unit, considering the aspects identified in the time-scale analysis and (iii) to mathematically prove all the results by applying the singular perturbation method.

In order to achieve these objectives, the current work exploits a representative DER-microgrid interaction model presented in Section 2.1 and apply the method of singular perturbation, described in Section 2.2. The mathematical proof of these results and the numerical simulations are presented in Sections 3 and 4. Finally, the conclusions of the analysis are drawn in Section 5.

Notation: $\mathbb{C}$ is the set of complex numbers, $\mathbb{R}$ is the set of real numbers and $\mathbb{R}^+$ is the set of real positive numbers. $\mathbb{R}^n$ denotes the n-dimensional Euclidean space and the operator $||.||$ represents the Euclidean norm. One-dimensional variables and functions are represented in italic lowercase letters. Multidimensional variables and functions (eg. vectors, complex numbers and vector valued functions) are written in bold lowercase letters. A n-dimensional variable being an argument of a function means that each projection can be represented as an argument of the same function, i.e., $f(t,\mathbf{v}) := f(t,v_1,\ldots,v_n), \mathbf{v} \in \mathbb{R}^n$.

2. Theoretical foundation

This section discusses the main concepts for the development of this study. Initially, the DER-microgrid interaction model is presented, and then the singular perturbation method is revisited.

2.1. DER-microgrid interaction model

A breakthrough in research on microgrid was achieved by [3], by exposing the precariousness of decoupled control based on the *droop* method. This fact led researchers to propose new control strategies to deal with microgrids, such as adaptive tilt controllers [12,13], synchronizers [4], virtual impedance [14] and others [15,16]. Much effort has been made in the study of new control strategies and synthesis; however, the central aspect of obtaining a successful controller is to find a suitable representative model.

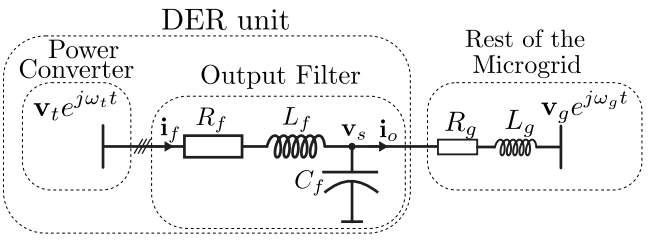

Fig. 1. Conventional structure of a DER unit connected to a microgrid.

The stability of a microgrid system is mainly determined by its primary (or decentralized) control integrated with each DER unit. The design of this controller must be based on the dynamic model that adequately describes the interaction between the DER unit and a microgrid. As the microgrids are a complex dynamic system, the use of a detailed model for control design purposes may be impractical. Despite these difficulties, some engineering aspects of the microgrid dynamic is assumed. A circuital model that represents the interaction between a DER unit and a microgrid is illustrated in Fig. 1. In this work, we consider the following assumptions regarding the microgrid, variable definitions, and model parameters, respectively.

Assumption 1. According to recent theoretical tendencies, a microgrid consists of a set of coupled oscillators [5,17,18], where the coupling is represented by transformers, filters, and distribution lines. In Fig. 1, the power converter represent an oscillator of adjustable voltage and frequency $\mathbf{v}_t e^{j\omega_t t}$, while the grid is also represented as an oscillator but the voltage and frequency are considered as exogenous variables, $\mathbf{v}_g e^{j\omega_g t}$.

Assumption 2. The state-space of the DER-microgrid interaction model is defined by the state variables $\mathbf{i}_f, \mathbf{v}_s, \mathbf{i}_o \in \mathbb{C}$ and $\delta \in \mathbb{R}$, where the angle δ represents the impact of the frequency deviation among oscillators. The input variables correspond to the voltage $\mathbf{v}_t \in \mathbb{C}$ and to the frequency $\omega_t \in \mathbb{R}$, which are considered as control degrees of freedom to be modulated at the converter terminal. Additionally, the voltage $\mathbf{v}_g \in \mathbb{C}$ and frequency $\omega_g \in \mathbb{R}$ of the oscillator that represents the microgrid are considered as unmeasured disturbances, which are mostly determined by the dynamic response of the network, loads, and other DER units. It is worth noting that, due to the uncertainties of these disturbances, their dynamics are not modeled. Instead, it can be assumed that they are bounded and belong to an assigned polytope D. This assumption is supported by the fact that (i) the variation on the power demand of the loads is neglectable under slight changes to the voltage amplitude and frequency of the network, and (ii) the control objective of the DER units within a microgrid is to regulate the voltage amplitude and frequency inside a defined region.

Assumption 3. It is assumed that the parameters of the filter that interfaces the power converter to the microgrid, $\{R_f, L_f, C_f\} \in \mathbb{R}$, are known with precision. On the other hand, the parameters that characterize the interconnection with microgrid, $\{R_g, L_g\} \in \mathbb{R}$, are subjected to uncertainties associated with the equivalent network impedance observed from the PoC of the DER unit.

The aforementioned assumptions relax, in two main aspects, the assumptions that the current literature, in general, adopts. First, the voltage and frequency $\{\mathbf{v}_g, \omega_g\}$ are typically considered fixed for control design purposes and disregards the effect of the angle δ that represents the oscillator behavior in the DER-microgrid interaction. However, the relevance of this variable on the dynamic model should not be disregarded as was documented in [19]. In contrast, in this study, $\{\mathbf{v}_g, \omega_g\}$ are assumed to be variables, enriching the dynamic model as adopting the Assumption 2. Secondly, a cascade control structure is commonly

adopted in the literature, where the filter $L_f C_f$ is considered by an internal feedback control [20,21] whereas the droop method deals with the outer control loop. In fact, it is a model reduction that has been criticized [6–9]. It is intended that the present work clarifies under which conditions the dynamic model of the output filter may or may not be reduced, in particular respect to the grid interaction (dominated by the angle δ). To this end, the open-loop response of the DER-microgrid interaction model is studied with the singular perturbation method.

The considered dynamic model is based on [3], which was used in [19] for control design purposes. The model in [19] is extended in this work to consider the dynamic model of the output filter presented in [22]. Note that the model here presented incorporates the mode of operation (grid-connected and islanded) in the disturbances $\mathbf{v}_g$ and ω_g as is considered in the Assumption 2. The set of differential equations are obtained as follows.

For an arbitrary rotary reference frame $\theta_t(t)$ with angular velocity $\omega_t(t) = d\theta_t(t)/dt$, the equations that describe the electrical circuit model in Fig. 1 can be expressed in the reference plane (*dq-frame*), which in general is adopted to be aligned with quadrature component of the capacitor voltage, regulating $v_{sq} = 0$ as

$$\frac{d\mathbf{i}_o}{dt} = -\frac{R_g}{L_g}\mathbf{i}_o - j\omega_t\mathbf{i}_o - \frac{\mathbf{v}_g}{L_g}e^{j\delta} + \frac{\mathbf{v}_s}{L_g}, \tag{1}$$

$$\frac{d\delta}{dt} = \omega_g - \omega_t, \tag{2}$$

$$\frac{d\mathbf{i}_f}{dt} = -\frac{R_f}{L_f}\mathbf{i}_f - j\omega_t\mathbf{i}_f - \frac{\mathbf{v}_s}{L_f} + \frac{\mathbf{v}_t}{L_f}, \tag{3}$$

$$\frac{d\mathbf{v}_s}{dt} = -\frac{\mathbf{i}_o}{C_f} - j\omega_t\mathbf{v}_s + \frac{\mathbf{i}_f}{C_f}. \tag{4}$$

There are mainly two aspects that require to be highlighted in this representation. First, in (2), δ is the integration of the frequency deviation between the exogenous disturbance ω_g and the frequency of the modulated voltage at the power converter terminal ω_t. Therefore, a small frequency deviation between oscillators the state δ tends to infinity and the full system is unstable in open-loop. Nonetheless, as will be seen, the singular perturbation method admits system models with this characteristic. Second, the parameters R_g and L_g condense the equivalent impedance of the network seen at the PoC of the DER unit. In this work, we consider that this equivalent impedance is dominated by the isolation transformer, which, for safety reason, is connected to interface the output filter to the microgrid. As a consequence, the equivalent network impedance is an additional source of uncertainty.

As can be seen, the DER-microgrid interaction model (1) - (4) has a nonlinear characteristic with uncertain parameters and unmodeled dynamics. As these differential equations are used to design the primary control of the DER units, before determining the control strategy, it is necessary to clarify the limitations and properties of the system. To that end, the fundamentals of singular perturbation theory are presented as follows, then it will be used for the DER-microgrid model in the next sections.

2.2. Singular Perturbation Method

The singular perturbation method aims for a dynamic model representation where the derivatives of some of the states are multiplied by a small parameter $\epsilon \in \mathbb{R}^+$ as

$$\dot{\mathbf{x}} = \mathbf{f}(t, \mathbf{x}, \mathbf{z}, \epsilon), \quad \mathbf{x}(t_0) = \mathbf{x}_0, \tag{5}$$

$$\epsilon\dot{\mathbf{z}} = \mathbf{g}(t, \mathbf{x}, \mathbf{z}, \epsilon), \quad \mathbf{z}(t_0) = \mathbf{z}_0, \tag{6}$$

where functions $\mathbf{f}, \mathbf{g}$ are Lipschitz and $(t, \mathbf{x}, \mathbf{z}, \epsilon) \in [0, \infty) \times \mathscr{D}_x \times \mathscr{D}_z \times [0, \epsilon_s]$, with $\mathscr{D}_x \subset \mathbb{R}^n$, $\mathscr{D}_z \subset \mathbb{R}^m$ and ϵ_s is the upper limit of the ϵ domain.

Our interest is to investigate the time-scale behavior of the solutions of (5) and (6) as $\epsilon \to 0$. Particularly, we wish to know the conditions that allow to neglect the parameter ϵ in the system given by (5) and (6), i.e. such that its solution can be approximated by a simplified system.

An order reduction in (5) and (6) is achieved when we set $\epsilon = 0$ in (6) and the dimension of the state equation changes from $n+m$ to n because (6) degenerates into the algebraic equations

$$\mathbf{0} = \mathbf{g}(t, \mathbf{x}, \mathbf{z}, 0), \tag{7}$$

which represents the so-called *slow manifold*.

To support this model reduction, the Tikhonov's Theorem should be stated. To that end, three assumptions must be made:

Assumption 4. Eq. (7) has at least an isolated real root with respect to variable $\mathbf{z}$, given by

$$\bar{\mathbf{z}} = \mathbf{h}(t, \mathbf{x}). \tag{8}$$

Eq. (8) represents the *quasi-steady state* of $\mathbf{z}$, ensuring that a well-defined n-dimensional reduced model will correspond to each root of (7).

The *reduced model* is obtained by replacing (8) in (5), with $\epsilon = 0$, as

$$\dot{\mathbf{x}} = \mathbf{f}(t, \mathbf{x}, \mathbf{h}(t, \mathbf{x}), 0), \tag{9}$$

and its solution is given by $\bar{\mathbf{x}}$.

Since (9) is a n-th order reduced model, we can only specify n initial conditions. Naturally, we retain the initial state, $\bar{\mathbf{x}}(t_0) = \mathbf{x}_0$ to obtain the reduced problem. On the other hand, the quasi-steady-state $\bar{\mathbf{z}}$ is not free to start from the same initial point of $\mathbf{z}$. Actually, there may be a large discrepancy between its initial value $\bar{\mathbf{z}}(t_0) = \mathbf{h}(t_0, \mathbf{x}_0)$ and the prescribed initial condition $\mathbf{z}(t_0) = \mathbf{z}_0$. Thus, $\bar{\mathbf{z}}$ cannot be an uniform approximation of $\mathbf{z}$. The best we can expect is that the approximation will hold on an interval excluding t_0 that is, for $t \in [t_1, T]$ where $t_1 > t_0$.

To analyze the behavior of $\mathbf{z}$ in the *boundary layer*, during the interval $t \in [t_0, t_1]$, we perform a change in the time-scale, given by

$$\tau = \frac{t - t_0}{\epsilon}, \tag{10}$$

where τ tends to infinity even for a fixed t, which could be slightly larger then t_0. Applying this new fast time-scale in (5) and (6), we obtain

$$\dot{\mathbf{x}} = \epsilon\mathbf{f}(\tau, \mathbf{x}, \mathbf{z}, \epsilon), \tag{11}$$

$$\dot{\mathbf{z}} = \mathbf{g}(\tau, \mathbf{x}, \mathbf{z}, \epsilon). \tag{12}$$

In a successful singular perturbation representation, for small ϵ, the right side of (11) also leads to small values. Thus, while $\mathbf{z}$ and τ almost instantaneously change, $\mathbf{x}$ remains very near its initial value $\mathbf{x}(t_0)$.

In order to describe the transient response of $\mathbf{z}$ around its steady state, we perform the change of variables $\mathbf{y} = \mathbf{z} - \mathbf{h}(t, \mathbf{x})$. In addition, to examine the response at the τ-time-scale, the change of variable $t = t_0 + \epsilon\tau$ is applied (5) and (6). Thus, the *boundary-layer model* is obtained as

$$\frac{d\mathbf{y}}{d\tau} = \mathbf{g}(t_0, \mathbf{x}_0, \mathbf{y} + \mathbf{h}(t_0, \mathbf{x}_0), 0), \tag{13}$$

$$\mathbf{y}(0) = \mathbf{z}_0 - \mathbf{h}(t_0, \mathbf{x}_0),$$

with t_0 and $\mathbf{x}_0$ fixed parameters and equilibrium at origin $\mathbf{y} = \mathbf{0}$.

We need a stability property that guarantees that $\mathbf{y}(\tau)$ will reach an neighborhood of the origin during the boundary-layer interval and, beyond this interval, will remain close to zero, while the slowly varying parameters $(t, \mathbf{x})$ move away from their initial values $(t_0, \mathbf{x}_0)$. For this, the *boundary-layer* general model (14) is used

$$\frac{d\mathbf{y}}{d\tau} = \mathbf{g}(t, \mathbf{x}, \mathbf{y} + \mathbf{h}(t, \mathbf{x}), 0). \tag{14}$$

The next two assumptions ensure a strong stability property of the

boundary layer model.

Assumption 5. The equilibrium $\mathbf{y}(\tau) = \mathbf{0}$ of (13) is asymptotically stable uniformly in $\mathbf{x}_0$ and t_0, and $\mathbf{z}_0 - \mathbf{h}(t_0, \mathbf{x}_0)$ belongs to its domain of attraction.

Assumption 6. The eigenvalues from the Jacobian Matrix $[\partial \mathbf{g}/\partial \mathbf{y}]$, along $\bar{\mathbf{x}}(t)$ and $\bar{\mathbf{z}}(t)$, in (14), have a real part less than a negative fixed number, i.e.

$$Re\left[\lambda\left\{\frac{\partial \mathbf{g}}{\partial \mathbf{y}}\right\}\right] \leqslant -c < 0. \tag{15}$$

Tikhonov's theorem establishes sufficient conditions that, after a certain time, the solutions of the perturbed model (5) and (6) have the same order of magnitude as those of the unperturbed model (8) and (9). Therefore, before to proceed with the Tikhonov's theorem, the concept of *order of magnitude* requires to be defined.

Definition 1. A vector function $\boldsymbol{\nu}(t, \epsilon) \in \mathbb{R}^n$ is said to have order of magnitude ϵ over an interval $[t_1, t_2]$, and we write $\boldsymbol{\nu}(t, \epsilon) = O(\epsilon)$, if there are positive values of k and ϵ^* such that

$$\|\nu(t, \epsilon)\| \leqslant k\epsilon, \forall \epsilon \in [0, \epsilon^*], \forall t \in [t_1, t_2]. \tag{16}$$

Theorem 1. (*[23] Theorem 3.1*) *Suppose the* Assumptions 4–6 *are satisfied. Then, for all* $t \in [t_0, T]$,

$$\mathbf{x}(t, \epsilon) - \bar{\mathbf{x}}(t) = O(\epsilon), \tag{17}$$

$$\mathbf{z}(t, \epsilon) - \mathbf{h}(t, \bar{\mathbf{x}}(t)) - \hat{\mathbf{y}}(t/\epsilon) = O(\epsilon) \tag{18}$$

and there is $t_1 \geqslant t_0$ *such that, for all* $t \in [t_1, T]$,

$$\mathbf{z}(t, \epsilon) - \mathbf{h}(t, \bar{\mathbf{x}}(t)) = O(\epsilon), \tag{19}$$

where $\bar{\mathbf{x}}$ *is the reduced model solution (9) and* $\hat{\mathbf{y}}$ *is the solution of the boundary layer model (13).* Tikhonov's theorem ensures the convergence of fast variables towards a slow surface for a limited period of time. It is important to highlight that this result also applies to an unstable open-loop model, as is the case of the DER-microgrid model presented in SubSection 2.1. The singular perturbation method is not compromised as we guarantee the stability of the slow manifold.

3. Singular Perturbation Method applied to the DER-Microgrid Model

In this section, the singular perturbation method presented in SubSection 2.2 is applied to the DER-microgrid model presented in SubSection 2.1. The main goal is to analyze the different time-scale of the variables involved in the interaction between a DER unit and a microgrid.

3.1. Open-loop analysis

The general form of singular perturbation in (5) and (6) is achieved by identifying a small constant ϵ that multiplies the time derivatives of some states. However, the parameter ϵ would be chosen as a ratio between physical parameters that reflects the smallness of ϵ in a relative sense. In addition, the variables and parameters of the differential equations should be formulated in terms of normalized variables, or dimensionless. Hence, the relative magnitude of each equation can be contrasted to its dimensionless coefficients, this procedure is known as *scaling* [24–27].

An essential task before using a perturbation scheme is to choose the state variables and time-scale that normalize the quantities. Hence, defining the voltage E and frequency ω_e as normalizing parameters, the next change of variable is performed, $\mathbf{x}_1 = \mathbf{i}_o R_g/E, x_2 = \delta, \mathbf{z}_1 = \mathbf{i}_f R_f/E$, $\mathbf{z}_2 = \mathbf{v}_s/E, \mathbf{u}_1 = \mathbf{v}_t/E, u_2 = \omega_t/\omega_e, \mathbf{w}_1 = \mathbf{v}_g/E$ and $w_2 = \omega_g/\omega_e$. As a consequence, the system Eqs. (1) - (4) are expressed in the state space representation, with coefficients and state variables written as dimensionless quantities with similar orders of magnitude, as recommended by [24]:

$$\frac{L_g}{R_g}\dot{\mathbf{x}}_1 = \mathbf{z}_2 - \mathbf{x}_1 - j\omega_e \frac{L_g}{R_g} u_2 \mathbf{x}_1 - \mathbf{w}_1 e^{jx_2}, \tag{20}$$

$$\frac{1}{\omega_e}\dot{x}_2 = -u_2 + w_2, \tag{21}$$

$$\frac{L_f}{R_f}\dot{\mathbf{z}}_1 = -\mathbf{z}_1 - j\omega_e \frac{L_f}{R_f} u_2 \mathbf{z}_1 - \mathbf{z}_2 + \mathbf{u}_1, \tag{22}$$

$$R_f C_f \dot{\mathbf{z}}_2 = \mathbf{z}_1 - j\omega_e R_f C_f u_2 \mathbf{z}_2 - \frac{R_f}{R_g}\mathbf{x}_1. \tag{23}$$

The complex variables of the differential Eqs. (20)–(23) can be separated into their real and imaginary components in order to obtain the equivalent 7-dimensional system of differential equations with real variables [28–30], with time constants $T_0 = 1/\omega_e, T_1 = L_g/R_g, T_2 = L_f/R_f$ and $T_3 = R_f C_f$, and a dimensionless time variable $t_r = t/T_1$, as follows [1]:

$$\dot{x}_{1d} = z_{2d} - x_{1d} + \frac{T_1}{T_0} u_2 x_{1q} - w_{1d}\cos x_2 + w_{1q}\sin x_2, \tag{24}$$

$$\dot{x}_{1q} = z_{2q} - x_{1q} - \frac{T_1}{T_0} u_2 x_{1d} - w_{1d}\sin x_2 - w_{1q}\cos x_2, \tag{25}$$

$$\dot{x}_2 = -\frac{T_1}{T_0}u_2 + \frac{T_1}{T_0}w_2, \tag{26}$$

$$\frac{T_2}{T_1}\dot{z}_{1d} = -z_{1d} + \frac{T_2}{T_0} u_2 z_{1q} - z_{2d} + u_{1d}, \tag{27}$$

$$\frac{T_2}{T_1}\dot{z}_{1q} = -z_{1q} - \frac{T_2}{T_0} u_2 z_{1d} - z_{2q} + u_{1q}, \tag{28}$$

$$\frac{T_3}{T_1}\dot{z}_{2d} = z_{1d} + \frac{T_3}{T_0} u_2 z_{2q} - \frac{R_f}{R_g} x_{1d}, \tag{29}$$

$$\frac{T_3}{T_1}\dot{z}_{2q} = z_{1q} - \frac{T_3}{T_0} u_2 z_{2d} - \frac{R_f}{R_g} x_{1q}. \tag{30}$$

According to the singular perturbation formulation in (5) and (6), the equations on the right side of (24)–(30) are called $f_{1d}, f_{1q}, f_2, g_{1d}, g_{1q}, g_{2d}$ and g_{2q}, respectively. In order to (24)–(30) be in the general form of singular perturbations, where $\mathbf{z}$ is much faster than $\mathbf{x}$, T_2 and T_3 must be *much smaller* than T_0 and T_1, i.e.,

$$\omega_e \frac{L_f}{R_f} \ll 1, \frac{L_f R_g}{L_g R_f} \ll 1, \tag{31}$$

$$\omega_e R_f C_f \ll 1, \frac{R_g R_f C_f}{L_g} \ll 1. \tag{32}$$

Assuming that the relationships in (31)–(32) are valid, the system (24)–(30) can be placed in the form of singular perturbations below, with multiple parameters of the same order [31]:

$$\dot{x}_{1d} = z_{2d} - x_{1d} + \alpha u_2 x_{1q} - w_{1d}\cos x_2 + w_{1q}\sin x_2, \tag{33}$$

$$\dot{x}_{1q} = z_{2q} - x_{1q} - \alpha u_2 x_{1d} - w_{1d}\sin x_2 - w_{1q}\cos x_2, \tag{34}$$

[1] From now on, the *reference time-scale* for this work is $t_r = t/T_1$. However, to simplify the notation, the subscript r will be omitted.

$$\dot{x}_2 = -\alpha u_2 + \alpha w_2, \tag{35}$$

$$\epsilon_1 \dot{z}_{1d} = -z_{1d} + \alpha \epsilon_1 u_2 z_{1q} - z_{2d} + u_{1d}, \tag{36}$$

$$\epsilon_1 \dot{z}_{1q} = -z_{1q} - \alpha \epsilon_1 u_2 z_{1d} - z_{2q} + u_{1q}, \tag{37}$$

$$\epsilon_2 \dot{z}_{2d} = z_{1d} + \alpha \epsilon_2 u_2 z_{2q} - R x_{1d}, \tag{38}$$

$$\epsilon_2 \dot{z}_{2q} = z_{1q} - \alpha \epsilon_2 u_2 z_{2d} - R x_{1q}, \tag{39}$$

with $\epsilon_1 = T_2/T_1, \epsilon_2 = T_3/T_1, \alpha = T_1/T_0$ and $R = R_f/R_g$. In order to normalize the expressions respect to a single parameter, ϵ_1 and ϵ_2 can be treated as proportional scalar, for example, $\epsilon = min\{\epsilon_1, \epsilon_2\}$ and $\epsilon_i = \beta_i \epsilon$, for $i = 1, 2$.

Following a proper DER unit output-filter design [32,33], it can be assumed that $T_3 \leqslant T_2$, then $\epsilon_2 < \epsilon_1$. Consequently, we can make $\epsilon = T_3/T_1$ and multiply both sides of (27) and (28) by $\beta = T_3/T_2$, to obtain the general form of singular perturbation for the open-loop DER-microgrid model:

$$\dot{x}_{1d} = z_{2d} - x_{1d} + \alpha u_2 x_{1q} - w_{1d}\cos x_2 + w_{1q}\sin x_2, \tag{40}$$

$$\dot{x}_{1q} = z_{2q} - x_{1q} - \alpha u_2 x_{1d} - w_{1d}\sin x_2 - w_{1q}\cos x_2, \tag{41}$$

$$\dot{x}_2 = -\alpha u_2 + \alpha w_2, \tag{42}$$

$$\epsilon \dot{z}_{1d} = -\beta z_{1d} + \alpha \epsilon u_2 z_{1q} - \beta z_{2d} + \beta u_{1d}, \tag{43}$$

$$\epsilon \dot{z}_{1q} = -\beta z_{1q} - \alpha \epsilon u_2 z_{1d} - \beta z_{2q} + \beta u_{1q}, \tag{44}$$

$$\epsilon \dot{z}_{2d} = z_{1d} + \alpha \epsilon u_2 z_{2q} - R x_{1d}, \tag{45}$$

$$\epsilon \dot{z}_{2q} = z_{1q} - \alpha \epsilon u_2 z_{2d} - R x_{1q}, \tag{46}$$

From this representation, the boundary-layer model $d\mathbf{y}/d\tau = \mathbf{g}(t, \mathbf{x}, \mathbf{y} + \mathbf{h}(t, \mathbf{x}), 0)$ for the system (40)–(46) is given by:

$$\dot{y}_{1d} = g_{1d}(t, \mathbf{x}, \mathbf{y} + \mathbf{h}(t, \mathbf{x}), 0) = -\beta y_{1d} - \beta y_{2d}, \tag{47}$$

$$\dot{y}_{1q} = g_{1q}(t, \mathbf{x}, \mathbf{y} + \mathbf{h}(t, \mathbf{x}), 0) = -\beta y_{1q} - \beta y_{2q}, \tag{48}$$

$$\dot{y}_{2d} = g_{2d}(t, \mathbf{x}, \mathbf{y} + \mathbf{h}(t, \mathbf{x}), 0) = y_{1d}, \tag{49}$$

$$\dot{y}_{2q} = g_{2q}(t, \mathbf{x}, \mathbf{y} + \mathbf{h}(t, \mathbf{x}), 0) = y_{1q}, \tag{50}$$

and its Jacobian matrix $[\partial \mathbf{g}/\partial \mathbf{y}]$ is given by:

$$J = \left[\frac{\partial \mathbf{g}}{\partial \mathbf{y}}\right] = \begin{bmatrix} -\beta & 0 & -\beta & 0 \\ 0 & -\beta & 0 & -\beta \\ 1 & 0 & 0 & 0 \\ 0 & 1 & 0 & 0 \end{bmatrix}. \tag{51}$$

Hence, the eigenvalue condition (15), given by $Re\left[\lambda\left\{\frac{\partial \mathbf{g}}{\partial \mathbf{y}}\right\}\right] < 0$, is then met for every $\beta > 0$.

Meeting the eigenvalue condition (51) means that the fast variables $\mathbf{z}_1$ and $\mathbf{z}_2$ of the system (40)–(46) converges exponentially to its quasi steady state $\mathbf{h}_1(t, \mathbf{x})$ and $\mathbf{h}_2(t, \mathbf{x})$. This quasi steady state is obtained for $\epsilon = 0$ in (43)–(46):

$$0 = -h_{1d}(t, \mathbf{x}) - h_{2d}(t, \mathbf{x}) + u_{1d}(t, \mathbf{x}, \mathbf{h}(t, \mathbf{x}), 0), \tag{52}$$

$$0 = -h_{1q}(t, \mathbf{x}) - h_{2q}(t, \mathbf{x}) + u_{1q}(t, \mathbf{x}, \mathbf{h}(t, \mathbf{x}), 0), \tag{53}$$

$$0 = h_{1d}(t, \mathbf{x}) - R x_{1d}, \tag{54}$$

$$0 = h_{1q}(t, \mathbf{x}) - R x_{1q}. \tag{55}$$

The *reduced model* is determined by replacing $\mathbf{h}_1$ and $\mathbf{h}_2$ obtained by (52)–(55) in (40)–(42):

$$\dot{x}_{1d} = u_{1d} - (1 + R)x_{1d} + \alpha u_2 x_{1q} - w_{1d}\cos x_2 + w_{1q}\sin x_2, \tag{56}$$

$$\dot{x}_{1q} = u_{1q} - (1 + R)x_{1q} - \alpha u_2 x_{1d} - w_{1q}\cos x_2 - w_{1d}\sin x_2, \tag{57}$$

$$\dot{x}_2 = -\alpha u_2 + \alpha w_2. \tag{58}$$

The solutions for $\mathbf{h}_1$ and $\mathbf{h}_2$ in (52)–(55) correspond to the surfaces where the variables $\mathbf{z}_1$ and $\mathbf{z}_2$ converge on a larger time-scale. Hence, in general terms, the problem of the reducing the system (40)–(46) also relies (in addition to the physical parameters) on the feedback design function $\mathbf{u}_1(t, \mathbf{x}, \mathbf{z}, \epsilon)$, as is seen in (52)–(55). It means that the relations (31)–(32) can be modified by using the input $\mathbf{u}_1$ to achieve the model reduction. Even though the accomplishment of these requirements relies on the output filter design, it is possible to empirically conclude, based on the low value of resistive cables characteristic, that (32) is met. However, the condition (31) is not evident (see [32,33] for practical design of the output filter).

In order to guarantee the separation of the time-scale between fast and slow variables, the next section presents the requirements for a feedback function $\mathbf{u}_1(t, \mathbf{x}, \mathbf{z}, \epsilon)$ such that (31) and (32) is fully satisfied.

3.2. Feedback control design requirements for model reduction

To ensure the applicability of the singular perturbation method in cases where the relationship (31) is not achieved, the state feedback control function $\mathbf{u}_1(t, \mathbf{x}, \mathbf{z}, \epsilon)$ in (43) and (44) must satisfy certain requirements.

Essentially, the influence of $\mathbf{u}_1(t, \mathbf{x}, \mathbf{z}, \epsilon)$ on the dynamic response of $\mathbf{f}(t, \mathbf{x}, \mathbf{z}, \epsilon)$ and $\mathbf{g}(t, \mathbf{x}, \mathbf{z}, \epsilon)$ in (24)–(30) – represented from now on by $\mathbf{f}_u(t, \mathbf{x}, \mathbf{z}, \epsilon)$ and $\mathbf{g}_u(t, \mathbf{x}, \mathbf{z}, \epsilon)$ – must be characterized on the singular perturbation formulation. Therefore, the first mandatory condition is to ensure the relative smallness of $\epsilon \mathbf{f}_u(\tau, \mathbf{x}, \mathbf{z}, \epsilon)$ in respect to $\mathbf{g}_u(\tau, \mathbf{x}, \mathbf{z}, \epsilon)$ in the fast time-scale, as in (11) and (12).

In particular, the separation between $\mathbf{g}_{1u}(\tau, \mathbf{x}, \mathbf{z}, \epsilon)$ and $\epsilon \mathbf{f}_{1u}(\tau, \mathbf{x}, \mathbf{z}, \epsilon)$ dynamics is achieved primarily from action on $\mathbf{z}_2$, which dominates both dynamics in the fast time-scale. In other words, we can get

$$||\mathbf{g}_{1u}(\tau, \mathbf{x}, \mathbf{z}, \epsilon)|| \geqslant \epsilon ||\mathbf{f}_{1u}(\tau, \mathbf{x}, \mathbf{z}, \epsilon)||, \tag{59}$$

by making the influence of $\mathbf{z}_2$ on $\mathbf{z}_1$ greater than on $\mathbf{x}_1$. It means that the feedback $\mathbf{u}_1(t, \mathbf{x}, \mathbf{z}, \epsilon)$ must associate a gain k_1 relatively to $\mathbf{z}_2$ in (27) and (28) such that $0 < T_2/(k_1 T_1) < 1$, leading to

$$k_1 > \frac{T_2}{T_1} \Rightarrow k_1 > \frac{L_f R_g}{R_f L_g}, \tag{60}$$

while reasonable gains associated with $\mathbf{z}_1$ and $\mathbf{x}_1$ can be used to others adjustments in the response.

In addition, the influence of each element on its own dynamics must be checked. In systems whose relations (31) and (32) are not sufficiently small, the terms $\alpha \epsilon u_2 \mathbf{z}_1$ and $\alpha \epsilon u_2 \mathbf{z}_2$ assume values that cannot be neglected in the slow timescale dynamics of (43)–(46). Thus, the influence of these terms must be eliminated through feedback.

An appropriate choice of $\mathbf{u}_1(t, \mathbf{x}, \mathbf{z}, \epsilon)$ also must ensure that $\mathbf{g}_{1u} = \mathbf{0}$ has unique solutions $\bar{\mathbf{z}}_1 = \mathbf{h}_1(t, \mathbf{x})$ and $\bar{\mathbf{z}}_2 = \mathbf{h}_2(t, \mathbf{x})$, meeting the Assumption 4, and the eigenvalue condition is satisfied for every $\mathbf{z}$ in the domain, i.e.

$$Re\left[\lambda\left\{\frac{\partial \mathbf{g}_u}{\partial \mathbf{z}}\right\}\right] < 0, \quad \forall \mathbf{z} \in D_z, \tag{61}$$

meeting the Assumptions 5 and 6.

Finally, the DER-microgrid interaction model can be reduced to:

$$\dot{x}_{1d} = h_{2d}(t, \mathbf{x}) - x_{1d} + \alpha u_2 x_{1q} - w_{1d}\cos x_2 + w_{1q}\sin x_2, \tag{62}$$

$$\dot{x}_{1q} = h_{2q}(t, \mathbf{x}) - x_{1q} - \alpha u_2 x_{1d} - w_{1q}\cos x_2 - w_{1d}\sin x_2, \tag{63}$$

$$\dot{x}_2 = -\alpha u_2 + \alpha w_2. \tag{64}$$

Now we present a proposal for the feedback control design. Let the control function $\mathbf{u}_1(t, \mathbf{x}, \mathbf{z}, \epsilon)$ be designed based on the procedure described above, in order to ensure the time-scale separation between $\mathbf{x}$ and $\mathbf{z}$ dynamic. To that end, the singular perturbation theory is used to the DER-microgrid interaction system. The feedback control law is represented as follows:

$$\mathbf{u}_1 = \mathbf{u}_F(t, \mathbf{x}, \mathbf{z}, \epsilon), \tag{65}$$

where $\mathbf{u}_F = (u_{Fd}, u_{Fq})$ is determined to ensure that the dynamics of $\mathbf{z}_1$ and $\mathbf{z}_2$ are faster than $\mathbf{x}_1$ and $\mathbf{x}_2$. From (27) and (28), $\mathbf{u}_F$ is chosen such that (59) and (60) are met:

$$u_{Fd} = (1-k_2)z_{1d} + (1-k_1)z_{2d} + k_1 z_{2d}^0 - \frac{\alpha\epsilon}{\beta} u_2 z_{1q} - k_2 \alpha \epsilon u_2 z_{2q} + k_2 R x_{1d}, \tag{66}$$

$$u_{Fq} = (1-k_2)z_{1q} + (1-k_1)z_{2q} + k_1 z_{2q}^0 + \frac{\alpha\epsilon}{\beta} u_2 z_{1d} + k_2 \alpha \epsilon u_2 z_{2d} + k_2 R x_{1q}. \tag{67}$$

where $\mathbf{z}_2^0$ is the reference signal of $\mathbf{z}_2$.

Then, evaluating (66) and (67) in the system model (33)–(39), the closed-loop system can be rewritten as:

$$\dot{x}_{1d} = z_{2d} - x_{1d} + \alpha u_2 x_{1q} - w_{1d}\cos x_2 + w_{1q}\sin x_2, \tag{68}$$

$$\dot{x}_{1q} = z_{2q} - x_{1q} - \alpha u_2 x_{1d} - w_{1q}\cos x_2 - w_{1d}\sin x_2, \tag{69}$$

$$\dot{x}_2 = -\alpha u_2 + \alpha w_2, \tag{70}$$

$$\epsilon \dot{z}_{1d} = -k_2\beta z_{1d} - k_1\beta z_{2d} + k_1\beta z_{2d}^0 - k_2\beta\alpha\epsilon u_2 z_{2q} + k_2\beta R x_{1d}, \tag{71}$$

$$\epsilon \dot{z}_{1q} = -k_2\beta z_{1q} - k_1\beta z_{2q} + k_1\beta z_{2q}^0 + k_2\beta\alpha\epsilon u_2 z_{2d} + k_2\beta R x_{1q}, \tag{72}$$

$$\epsilon \dot{z}_{2d} = z_{1d} + \alpha\epsilon u_2 z_{2q} - R x_{1d}, \tag{73}$$

$$\epsilon \dot{z}_{2q} = z_{1q} - \alpha\epsilon u_2 z_{2d} - R x_{1q}. \tag{74}$$

By setting $\epsilon = 0$ in. (71)–(74), the *quasi-stationary state* of $\mathbf{z}$, can be obtained (as aforementioned, the terms $\alpha\epsilon u_2 \mathbf{z}_1$ and $\alpha\epsilon u_2 \mathbf{z}_2$ cannot be neglected):

$$h_{1d}(t, \mathbf{x}) = -\alpha\epsilon u_2 z_{2q}^0 + R x_{1d}, \tag{75}$$

$$h_{1q}(t, \mathbf{x}) = \alpha\epsilon u_2 z_{2d}^0 + R x_{1q}, \tag{76}$$

$$h_{2d}(t, \mathbf{x}) = z_{2d}^0, \tag{77}$$

$$h_{2q}(t, \mathbf{x}) = z_{2q}^0. \tag{78}$$

And the boundary-layer model for the system (68)–(74) is given by:

$$\dot{y}_{1d} = g_{1ud}(t, \mathbf{x}, \mathbf{y} + \mathbf{h}(t, \mathbf{x}), 0) = -k_2\beta y_{1d} - k_1\beta y_{2d} - k_2\beta\alpha\epsilon u_2 y_{2q}, \tag{79}$$

$$\dot{y}_{1q} = g_{1uq}(t, \mathbf{x}, \mathbf{y} + \mathbf{h}(t, \mathbf{x}), 0) = -k_2\beta y_{1q} - k_1\beta y_{2q} + k_2\beta\alpha\epsilon u_2 y_{2d}, \tag{80}$$

$$\dot{y}_{2d} = g_{2d}(t, \mathbf{x}, \mathbf{y} + \mathbf{h}(t, \mathbf{x}), 0) = y_{1d} + \alpha\epsilon u_2 y_{2q}, \tag{81}$$

$$\dot{y}_{2q} = g_{2q}(t, \mathbf{x}, \mathbf{y} + \mathbf{h}(t, \mathbf{x}), 0) = y_{1q} - \alpha\epsilon u_2 y_{2d}, \tag{82}$$

and its Jacobian matrix $[\partial \mathbf{g}/\partial \mathbf{y}]$ is given by:

$$J = \left[\frac{\partial \mathbf{g}}{\partial \mathbf{y}}\right] = \begin{bmatrix} -k_2\beta & 0 & -k_1\beta & -k_2\beta\alpha\epsilon u_2 \\ 0 & -k_2\beta & k_2\beta\alpha\epsilon u_2 & -k_1\beta \\ 1 & 0 & 0 & \alpha\epsilon u_2 \\ 0 & 1 & -\alpha\epsilon u_2 & 0 \end{bmatrix} \tag{83}$$

and then the eigenvalue condition (15) is met for every real positives k_1, $k_2, \alpha, \beta, \epsilon$ and u_2.

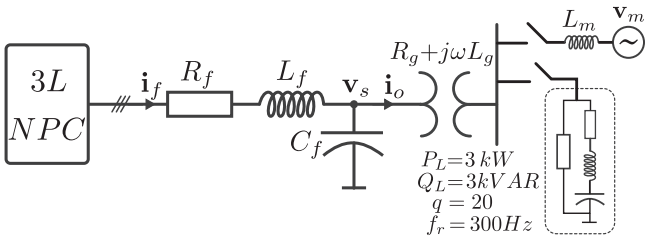

Fig. 2. Simulation test system under study.

Table 1
Output filter parameters.

Filter	Parameter
1	$R_{f1} = 92.5m\Omega, L_{f1} = 77\mu H, C_{f1} = 30\mu F$
2	$R_{f2} = 92.5m\Omega, L_{f2} = 770\mu H, C_{f2} = 30\mu F$

Finally, the *reduced model* is determined by replacing (75)–(78) in (68)–(70):

$$\dot{x}_{1d} = -x_{1d} + \alpha u_2 x_{1q} + z_{2d}^0 - w_{1d}\cos x_2 + w_{1q}\sin x_2, \tag{84}$$

$$\dot{x}_{1q} = -x_{1q} - \alpha u_2 x_{1d} + z_{2q}^0 - w_{1q}\cos x_2 - w_{1d}\sin x_2, \tag{85}$$

$$\dot{x}_2 = -\alpha u_2 + \alpha w_2. \tag{86}$$

The above result establishes that if the feedback law $\mathbf{u}_1$ is chosen as (66) and (67), the DER-microgrid dynamic model can be reduced to (84)–(86). The Assumptions 4–6 are accomplished and Theorem 1 confirms the model reduction.

4. Numerical results

This section presents two case studies that illustrate the practical use of the theoretical results obtained in this study. First, the parametric conditions (31) and (32) are certified in two sets of output filter parameters, showing that those conditions effectively determine if the output filter can be reduced in open-loop. The second case study shows the effectiveness of the feedback control law (66) and (67) to satisfy the reduction conditions. Both case studies are consistent with analytical results presented in this work and with the Theorem 1. To those ends, the dynamics of the current $\mathbf{i}_o$ of the reduced model is compared with the current $\mathbf{i}_o$ of the complete model. The test system is illustrated in Fig. 2, it is designed for a nominal power of $20kVA$ and it is simulated in the PSCAD/EMTDC software. The power converter corresponds to a three-level neutral point clamped (NPC) with a frequency modulation of $20kHz$ and fundamental frequency $\omega_c = 2\pi 60$. In Fig. 2, the DER unit is subject to the connection of a resonant load and to the connection of the main grid. The islanding transformer is characterized by the parameters $R_g = 0.44\,\Omega$ and $L_g = 2mH$ and the main grid by the inductance $L_m = 3mH$ and voltage $\mathbf{v}_m = 0.38\,kV$ with frequency $\omega_g = 2\pi 60$.

4.1. Case Study 1. Open-loop model reduction

Concerning the analytical conditions that authorize the open-loop model reduction (31) and (32), this case study considers two sets of parameters for the output filter ($R_f L_f C_f$) which are presented in Table 1.

The set of parameters for the Filter '1' has been chosen to satisfy the conditions (31) and (32) by decreasing the inductance L_f of the filter. However, the reduction of L_f reduces the range of the filter attenuation to high-frequency components of the modulated converter voltage. For that reason, the inductance L_f is increased for the output Filter '2' providing a filtering characteristic for the current $\mathbf{i}_f$ and voltage $\mathbf{v}_s$ of the DER unit. Unfortunately, increasing L_f compromises the achievement of

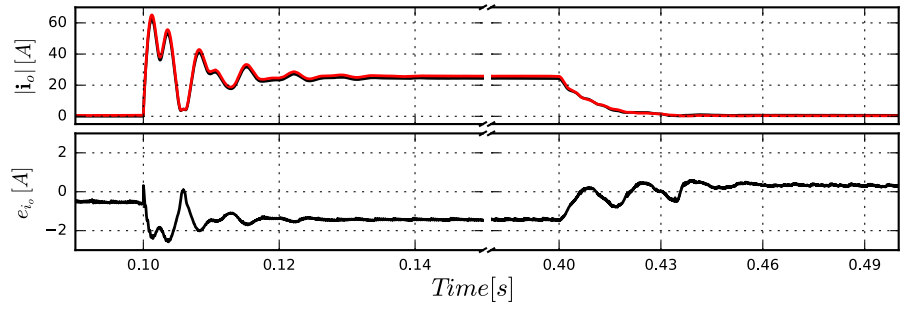

(a) Complete model (black-lines) and reduced (red-line) with Filter '1' that satisfy the reduction condition in open-loop. Response to load connection at $t = 0.1\,s$ and grid-connected transition at $t = 0.4\,s$.

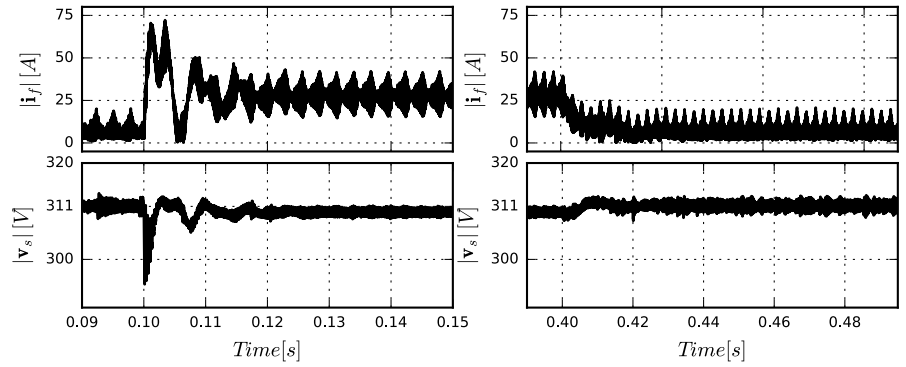

(b) Current $\mathbf{i}_f$ and voltage $\mathbf{v}_s$ response of the Filter '1' that satisfies the model reduction. Response to load connection at $t = 0.1\,s$ and grid-connected transition at $t = 0.4\,s$.

Fig. 3. Open loop dynamics for Filter '1'.

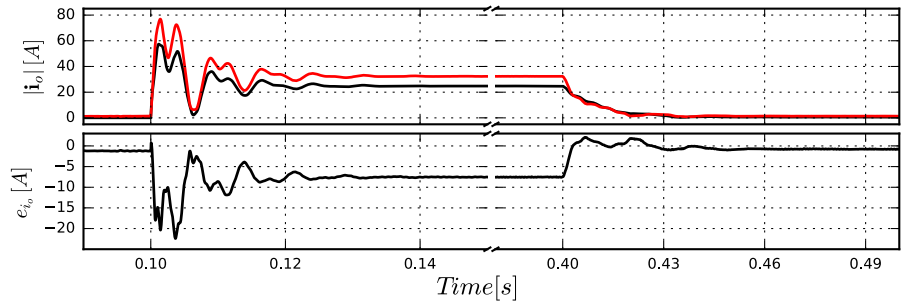

(a) Complete model (black-lines) and reduced (red-line) with Filter '2' that fails the reduction condition in open-loop. Response to load connection at $t = 0.1\,s$ and grid-connected transition at $t = 0.4\,s$.

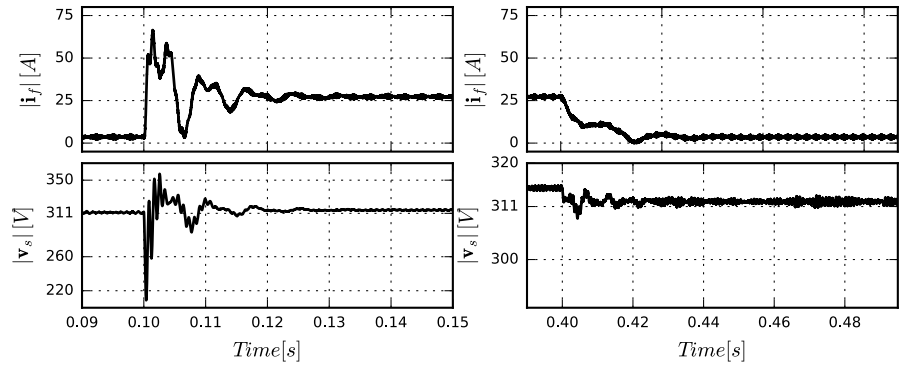

(b) Current $\mathbf{i}_f$ and voltage $\mathbf{v}_s$ response of the Filter '2' that fails the model reduction conditions. Response to load connection at $t = 0.1\,s$ and grid-connected transition at $t = 0.4\,s$.

Fig. 4. Open loop dynamics for Filter '2'.

reduction conditions (31) and (32).

In Fig. 3 and 4, the dynamic response of the current $\mathbf{i}_o$ for the complete (black-color lines) and reduced model (red-color lines) are illustrated for Filter '1' and Filter '2', respectively. In both figures, the error between the complete and the reduced model response are also depicted, $e_{i_o} = \left|\mathbf{i}_o(t)\right| - \left|\mathbf{i}_o^{red}(t)\right|$. At $t = 0.1\,s$ the resonant load is connected and at $t = 0.4\,s$ the main grid is connected, see Fig. 2. Fig. 3(a) presents the model reduction based on Filter '1' that satisfies the reduction conditions. In this figure, the reduced model exhibits good approximation respect to the complete dynamic model. For the case where the filter fails the reduction conditions, in Fig. 4(a), the transient and steady-state errors are evident. However, since the Filter '1' parameters (which satisfy the reduction conditions) exhibit low attenuation of the high-frequency components, the effect of the voltage modulation is perceived in the current $\mathbf{i}_f$ and voltage $\mathbf{v}_s$ as illustrated in Fig. 3(b). Therefore, this filter design is not applicable in a real implementation. Nonetheless, for the Filter '2' the attenuation of the high-frequency component is suitable as shown in Fig. 4(b), but it fails the reduction conditions. Hence, to successfully achieve a representative reduced model, a feedback law design is required, as is presented in the next case study.

4.2. Case Study 2. Closed-loop model reductions

This case study implements the feedback law proposed in (66) and (67) to accomplish the singular perturbation requirements (60) for the closed-loop system. Considering the output Filter '2' parameters, the relationship $T_2/T_1 = 2.4$ in (60) and consequently k_1 is chosen as $k_1 = 5$. On the other hand, k_2 is chosen to be $k_2 = 60$. The same events in the previous case study are presented in this section. In Fig. 5(a) the response of the closed-loop system is depicted in black-color line and the response of the reduced model (84)–(86) in red-color line. As can be seen, the reduced model effectively follows the real dynamic of the system with a small error, around 3% of the maximum current. On the other hand, the filtering characteristic of the filter is suitable and exhibits a fast dynamic response under the presented incidents, as is illustrated in Fig. 5(b).

5. Conclusion

The singular perturbations method was applied to the dynamic model that characterizes the interaction between a DER unit and a microgrid. This analysis shows that the timescale responses associated with the output filter and the rest of the microgrid are not sufficiently separated to allow a direct order reduction of the system. Nonetheless, it was also shown that if a feedback law satisfies a certain parametric condition, the order reduction of the dynamic model is authorized. As a consequence, the dynamic model that describes the interaction between a DER unit and the microgrid can be reduced for control design purposes.

CRediT authorship contribution statement

Bruno Salgado Bizzo: Methodology, Formal analysis, Writing - original draft, Software, Validation, Conceptualization, Visualization, Writing - review & editing. **Guilherme Araujo Pimentel:** Methodology, Formal analysis, Writing - original draft, Conceptualization, Conceptualization, Visualization, Writing - review & editing, Supervision. **Rafael da Silveira Castro:** Writing - original draft, Writing - review & editing. **Ricardo Pérez-Ibacache:** Methodology, Formal analysis, Writing -

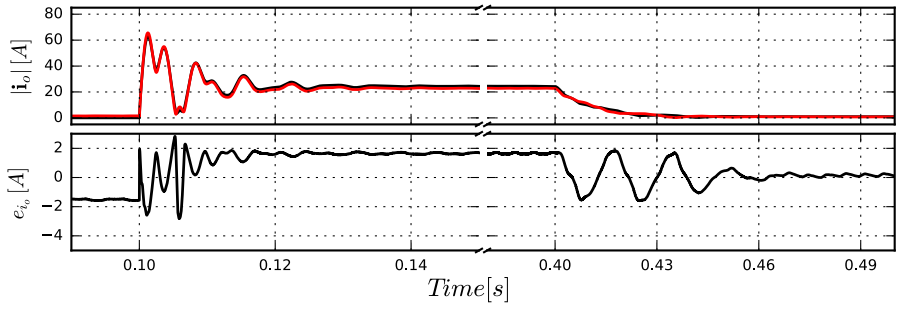

(a) Complete model (black-lines) and reduced (red-line) with filter parameters '2' in closed-loop. Response to load connection at $t = 0.1\,s$ and grid-connected transition at $t = 0.4\,s$.

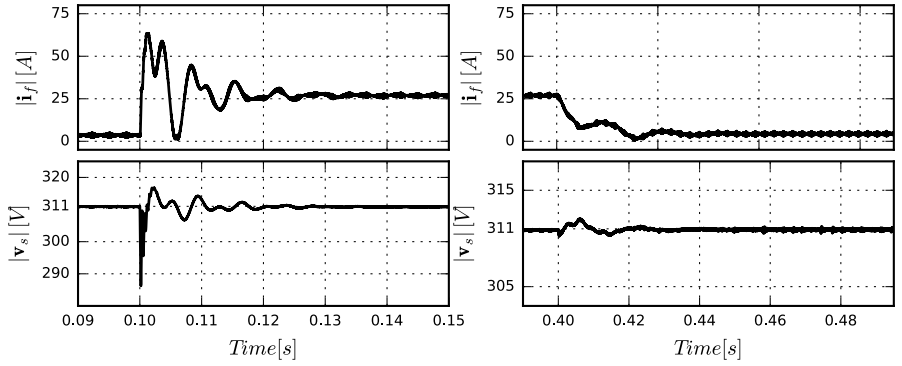

(b) Current $\mathbf{i}_f$ and voltage $\mathbf{v}_s$ response of the Filter '2' in closed-loop. Response to load connection at $t = 0.1\,s$ and grid-connected transition at $t = 0.4\,s$

Fig. 5. Closed loop dynamics for Filter '2'.

original draft, Software, Validation, Conceptualization, Visualization, Writing - review & editing.

Declaration of Competing Interest

The authors declare that they have no known competing financial interests or personal relationships that could have appeared to influence the work reported in this paper.

Acknowledgement

The authors acknowledge the computational support of CCTVal (ANID PIA/APOYO AFB180002) for this research. This work was supported in part by the Coordenação de Aperfeiçoamento De Pessoal de Nível Superior–Brasil (CAPES)–Finance Code 001.

References

[1] Chow JH, editor. Time-scale modeling of dynamic networks with applications to power systems. Springer-Verlag; 1982.
[2] Kundur P, Balu NJ, Lauby MG. Power system stability and control, vol. 7. New York: McGraw-Hill; 1994.
[3] Pogaku N, Prodanovic M, Green TC. Modeling, analysis and testing of autonomous operation of an inverter-based microgrid. IEEE Trans Power Eectron 2007;22(2):613–25.
[4] Zhong Q-C, Weiss G. Synchronverters: Inverters that mimic synchronous generators. IEEE Trans Industr Electron 2010;58(4):1259–67.
[5] Dorfler F, Chertkov M, Bullo F. Synchronization in complex oscillator networks and smart grids. Proc Nat Acad Sci 2013;110(6):2005–10.
[6] Yuan Z, Du Z, Li C, An T. Dynamic equivalent model of vsc based on singular perturbation. IET Generat Transmis Distrib 2016;10(14):3413–22.
[7] Gu Y, Bottrell N, Green TC. Reduced-order models for representing converters in power system studies. IEEE Trans Power Electron 2017;33(4):3644–54.
[8] Liao S, Zha X, Li X, Huang M, Sun J, Pan J, Guerrero JM. A novel dynamic aggregation modeling method of grid-connected inverters: Application in small-signal analysis. IEEE Trans Sustainable Energy 2019;10(3):1554–64.
[9] Purba V, Johnson BB, Rodriguez M, Jafarpour S, Bullo F, Dhople SV. Reduced-order aggregate model for parallel-connected single-phase inverters. IEEE Trans Energy Convers 2018;34(2):824–37.
[10] Khalil HK. Noninear systems. 3rd ed. New Jersey: Prentice-Hall; 2002.
[11] Strogatz SH. Exploring complex networks. Nature 2001;410(6825):268–76.
[12] Mohamed YA-RI, El-Saadany EF. Adaptive decentralized droop controller to preserve power sharing stability of paralleled inverters in distributed generation microgrids. IEEE Trans Power Electron 2008;23(6):2806–16.
[13] Delghavi MB, Yazdani A. An adaptive feedforward compensation for stability enhancement in droop-controlled inverter-based microgrids. IEEE Trans Power Deliv 2011;26(3):1764–73.
[14] Kim J, Guerrero JM, Rodriguez P, Teodorescu R, Nam K. Mode adaptive droop control with virtual output impedances for an inverter-based flexible ac microgrid. IEEE Trans Power Electron 2010;26(3):689–701.
[15] Morstyn T, Hredzak B, Agelidis VG. Control strategies for microgrids with distributed energy storage systems: An overview. IEEE Trans Smart Grid 2016;9(4):3652–66.
[16] Sen S, Kumar V. Microgrid control: A comprehensive survey. Ann Rev Control 2018;45:118–51.
[17] Simpson-Porco JW, Dorfler F, Bullo F. Synchronization and power sharing for droop-controlled inverters in islanded microgrids. Automatica 2013;49(9):2603–11.
[18] Zhu L, Hill DJ. Synchronization of kuramoto oscillators: A regional stability framework. IEEE Trans Autom Control 2020;65(12):5070–82.
[19] Perez-Ibacache R, Silva CA, Yazdani A. Linear state-feedback primary control for enhanced dynamic response of ac microgrids. IEEE Trans Smart Grid 2018;10(3):3149–61.
[20] Han H, Hou X, Yang J, Wu J, Su M, Guerrero JM. Review of power sharing control strategies for islanding operation of ac microgrids. IEEE Trans Smart Grid 2015;7(1):200–15.
[21] Tayab UB, Roslan MAB, Hwai LJ, Kashif M. A review of droop control techniques for microgrid. Renew Sustain Energy Rev 2017;76:717–27.
[22] Sadabadi MS, Haddadi A, Karimi H, Karimi A. A robust active damping control strategy for an lcl -based grid-connected dg unit. IEEE Trans Industr Electron 2017;64(10):8055–65.
[23] Kokotović P, Khalil HK, O'Reilly J. Singular perturbation methods in control: analysis and design. Society for Industrial and Applied Mathematics; 1999.

[24] Lin CC, Segel LA. Mathematics applied to deterministic problems in the natural sciences. Society for Industrial and Applied Mathematics; 1988.
[25] Logan J. Applied Mathematics. 4th ed. Wiley; 2013.
[26] Rienstra SW. Modelling and perturbation methods. Tech. rep., Eindhoven University of Technology, 2002.
[27] Shchepakina E, Sobolev V, Mortell MP. Singular perturbations: introduction to system order reduction methods with applications, vol. 2114. Springer; 2014.
[28] Battelli F, Fevckan M. Handbook of differential equations: ordinary differential equations. Elsevier; 2008.
[29] Testard L. Visualization of complex ODE solutions. In: Mathematical Visualization. Springer; 1998. p. 353–62.
[30] Schreier PJ, Scharf LL. Statistical signal processing of complex-valued data: the theory of improper and noncircular signals. Cambridge University Press; 2010.
[31] Khalil HK. Asymptotic stability of nonlinear multiparameter singularly perturbed systems. Automatica 1981;17(6):797–804.
[32] Liserre M, Blaabjerg F, Hansen S. Design and control of an lcl-filter-based three-phase active rectifier. IEEE Trans Ind Appl 2005;41(5):1281–91.
[33] Said-Romdhane M, Naouar M, Belkhodja I, Monmasson E. An improved lcl filter design in order to ensure stability without damping and despite large grid impedance variations. Energies 2017;10(336):1–19.